Title

Ultrasensitive version of nucleic acid sequence-based amplification (NASBA) utilizing a nicking and extension chain reaction system

Journal

Nanoscale, 13(24)

ISSN

2040-3364

Authors

Ju, Yong
Kim, Hyo Yong
Ahn, Jun Ki
et al.

Publication Date

2021-06-24

DOI

10.1039/d1nr00564b

Volume 13
Number 24
28 June 2021
Pages 10613-10954

Nanoscale

rsc.li/nanoscale

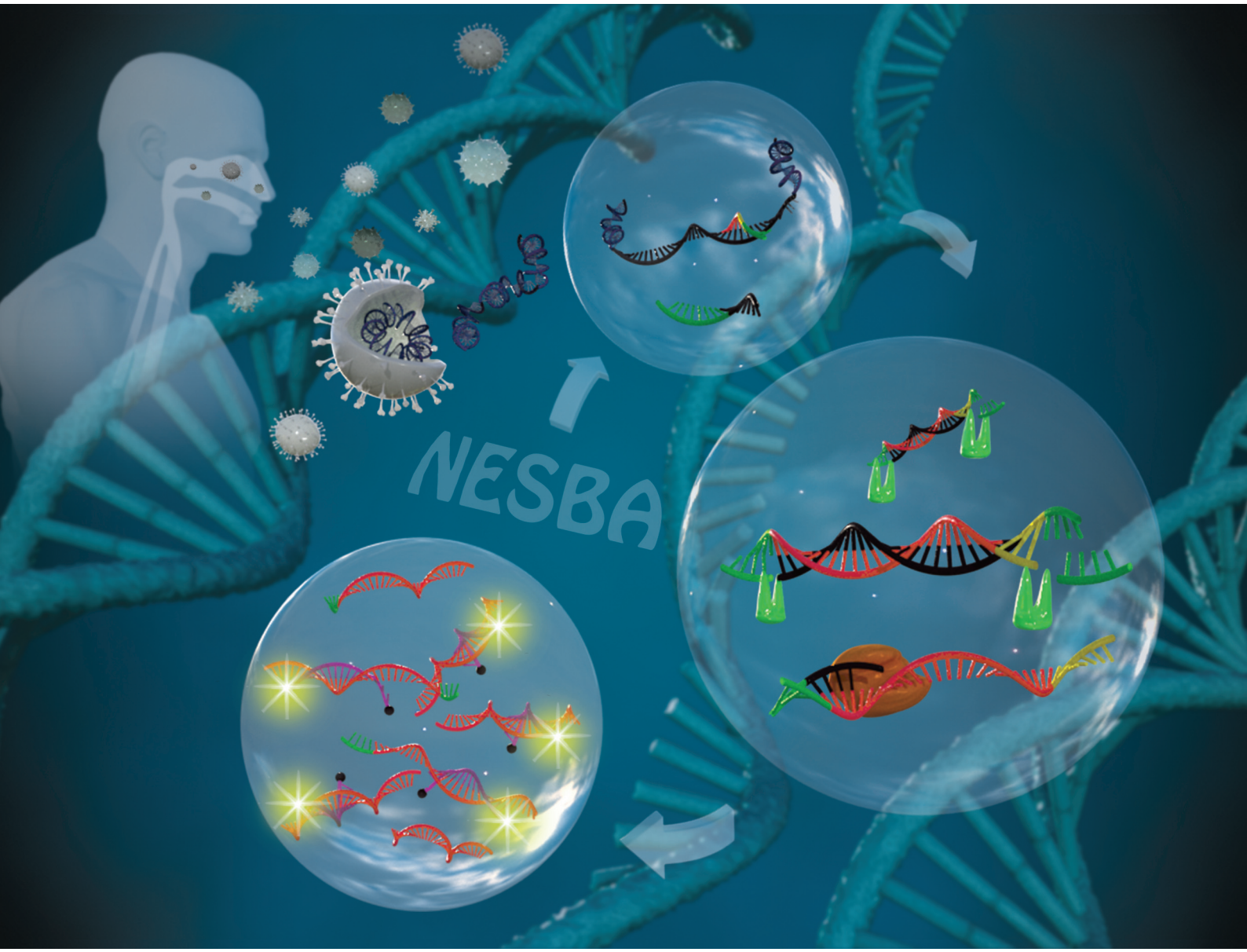

ISSN 2040-3372

ROYAL SOCIETY OF CHEMISTRY

PAPER

Hyun Gyu Park *et al.*

Ultrasensitive version of nucleic acid sequence-based amplification (NASBA) utilizing a nicking and extension chain reaction system

NCNST

Nanoscale

PAPER

View Article Online
View Journal | View Issue

Cite this: *Nanoscale*, 2021, **13**, 10785

Ultrasensitive version of nucleic acid sequence-based amplification (NASBA) utilizing a nicking and extension chain reaction system†

Yong Ju,‡[a] Hyo Yong Kim,‡[a] Jun Ki Ahn[a,b] and Hyun Gyu Park *[a]

Received 26th January 2021,
Accepted 9th May 2021

DOI: 10.1039/d1nr00564b

rsc.li/nanoscale

Nucleic acid sequence-based amplification (NASBA) is a transcription-based isothermal amplification technique especially designed for the detection of RNA targets. The NASBA basically relies on the linear production of T7 RNA promoter-containing double-stranded DNA (T7DNA), and thus the final amplification efficiency is not sufficiently high enough to achieve ultrasensitive detection. We herein ingeniously integrate a nicking and extension chain reaction system into the NASBA to establish an ultrasensitive version of NASBA, termed Nicking and Extension chain reaction System-Based Amplification (NESBA). By employing a NESBA primer set designed to contain an additional nicking site at the 5′ end of a NASBA primer set, the T7DNA is exponentially amplified through continuously repeated nicking and extension chain reaction by the combined activities of nicking endonuclease (NE) and reverse transcriptase (RT). As a consequence, a much larger number of RNA amplicons would be produced through the transcription of the amplified T7DNA, greatly enhancing the final fluorescence signal from the molecular beacon (MB) probe binding to the RNA amplicon. Based on this unique design principle, we successfully identified the target respiratory syncytial virus A (RSV A) genomic RNA (gRNA) down to 1 aM under isothermal conditions, which is 100-fold more sensitive than regular NASBA.

Introduction

Over the past few decades, isothermal amplification techniques have shown great promise by serving as an alternative technique to conventional PCR method due to their several intrinsic merits including low hardware dependence and rapid amplification.[1–3] Since these advantageous features of the isothermal strategy are very critical to realize point-of-care (POC) or on-site nucleic acid detection in resource-limited environments, various isothermal amplification methods such as loop-mediated amplification (LAMP),[4–8] strand displacement amplification (SDA),[9–11] helicase-dependent amplification (HDA),[12–14] rolling circle amplification (RCA),[15–17] recombinase polymerase amplification (RPA),[18,19] isothermal chain amplification (ICA),[20,21] exponential amplification reaction (EXPAR),[22,23] nucleic acid sequence-based amplification (NASBA),[24–26] and so on[27–30] have been extensively developed.

Of these, NASBA is the only isothermal strategy designed to detect genomic RNA (gRNA) targets, while almost all the other methods are intended to identify double-stranded DNA targets.[31–34] In the NASBA, the presence of target RNA triggers the formation of T7 RNA promoter-containing double-stranded DNA (T7DNA) through the combined activities of reverse transcriptase (RT) and RNase H. T7 RNA polymerase (T7RP) then promotes the transcription from the T7 RNA promoter region within the T7DNA, consequently producing numerous antisense RNA amplicons. The RNA amplicon also serves as a template to produce another T7DNA in the similar manner to the original gRNA, further accelerating the isothermal amplification of RNA amplicons. The produced RNA amplicons are finally monitored by employing molecular beacons (MBs), which could produce highly fluorescent signal upon binding to the RNA amplicons. By relying on this design principle, the NASBA has served as the most powerful method to identify gRNA targets under an isothermal condition and has been extensively applied for the diagnosis of RNA virus infections.[31,35–37] Notably, several diagnostic kits to identify SARS-CoV-2 virus have been recently developed and commercialized based on the NASBA technology in the current ongoing pandemic of COVID-19.[38,39] The key intermediate

[a]*Department of Chemical and Biomolecular Engineering (BK21+ Program), Korea Advanced Institute of Science and Technology (KAIST), 291 Daehak-ro, Yuseong-gu, Daejeon 34141, Republic of Korea. E-mail: hgpark@kaist.ac.kr; Fax: +82-42-350-3910; Tel: +82-42-350-3932*

[b]*Human Convergence Technology Group, Korea Institute of Industrial Technology (KITECH), 143 Hanggaul-ro, Sangnok-gu, Ansan 15588, Republic of Korea*

†Electronic supplementary information (ESI) available. See DOI: 10.1039/d1nr00564b

‡These authors equally contributed to this work.

component of NASBA, T7DNA, however, is just linearly produced but not in an exponential manner and thus the final amplification efficiency is not sufficiently high enough to enable highly sensitive detection of target RNA, which might lead to false-negative results.[40,41]

Based on this background, we herein developed an advanced ultrasensitive version of NASBA, called Nicking and Extension chain reaction System-Based Amplification (NESBA) by ingeniously incorporating a nicking and extension chain reaction into the NASBA method. With the NESBA technique, we successfully identified the target gRNA extracted from respiratory syncytial virus A (RSV A) down to 1 aM, which is not feasible with the conventional NASBA method.

Experimental

Materials

All DNA oligonucleotides used in this study were synthesized and purified by high performance liquid chromatography (HPLC) using Bioneer® (Daejeon, Korea). The sequences of the oligonucleotides are listed in Table S1.† Nt.AlwI, 10× NEBuffer™ 2.1 (100 mM Tris-HCl, pH 7.9, 500 mM NaCl, 100 mM $MgCl_2$, and 1 mg ml^{-1} BSA), ribonucleotide solution mixture (rNTPs), and deoxynucleotide solution mixture (dNTPs) were purchased from New England Biolabs Inc. (Beverly, MA, USA). NASBA enzyme cocktail (avian myeloblastosis virus reverse transcriptase (AMV RT), RNase H, and T7 RNA polymerase (T7RP) in a high molecular weight sugar matrix) and 3× NASBA reaction buffer (120 mM Tris-HCl, pH 8.5, 210 mM KCl, 36 mM $MgCl_2$, 30 mM DTT, and 45% DMSO) were purchased from Life Science Advanced Technologies Inc. (St Petersburg, FL, USA). RevertAid RT reverse transcription kit was purchased from Thermo Fisher Scientific (Waltham, MA, USA). i-StarMAX™ II PCR kit was purchased from iNtRON Biotechnology Inc. (Daejeon, Korea). ATCC VR-26 (RSV A), KUMC-42 (RSV B), A/Brisbane/10/2007 (H3N2), A/equine/Kyonggi/SA1/2011 (H3N8), A/California/07/2009 (H1N1), A/swine/Korea/GC0502/2005 (H1N2), and A/aquatic bird/Korea/CN2-MA/2009 (H5N2) viruses were provided by the Korea Research Institute of Bioscience and Biotechnology (KRIBB, Daejeon, Korea). Ultrapure DNase/RNase-free distilled water (DW) was purchased from Bioneer® and used in all experiments. All other chemicals were of analytical grade and used without further purification.

gRNA extraction

The gRNAs were extracted from ATCC VR-26 (RSV A), KUMC-42 (RSV B), A/Brisbane/10/2007 (H3N2), A/equine/Kyonggi/SA1/2011 (H3N8), A/California/07/2009 (H1N1), A/swine/Korea/GC0502/2005 (H1N2), and A/aquatic bird/Korea/CN2-MA/2009 (H5N2) viruses by using QIAamp Viral RNA Mini kit (Qiagen, Hilden, Germany) according to the manufacturer's protocol. The concentrations of the extracted gRNAs were determined by using a NanoDrop™ 1000 spectrophotometer (Thermo Fisher Scientific, MA, USA). The extracted gRNAs were stored at −20 °C before use.

The NESBA procedure for target gRNA detection

30 μM MB solution was prepared in 1× NESBA reaction buffer (45 mM Tris-HCl (pH 8.5), 70 mM KCl, 25 mM NaCl, 17 mM $MgCl_2$, 10 mM DTT, 15% DMSO, and 50 μg mL^{-1} BSA) by using MB stock solution. The prepared MB solution was then heated up to 95 °C for 5 min, followed by slow cooling down to 25 °C, and was further incubated at 25 °C for 30 min.

The NESBA solution was next prepared by mixing two separately prepared solutions, solution A and B. The solution A (14.5 μL) prepared by mixing 2.8 μL rNTPs (25 mM each), 1.4 μL dNTPs (10 mM each), 1.4 μL NESBA primer set (20 μM each), 0.2 μL MB (30 μM), 7.7 μL NESBA reaction buffer (2.6×), and 1 μL gRNA solution at varying concentrations was heated up to 65 °C for 5 min, followed by slow cooling down to 41 °C, and was further incubated at 41 °C for 5 min. The solution B (5.5 μL) containing 5 μL NASBA enzyme cocktail (4×) and 0.5 μL Nt.AlwI (10 U μL^{-1}) was added to the solution A. The mixed NESBA solution (20 μL) was incubated at 41 °C for 1 h during which the fluorescence signal from MB was measured every 1 min by using a CFX Connect™ Real-Time System (Bio-Rad, CA, USA).

The NASBA procedure for target gRNA detection

The NASBA reaction was conducted by following the manufacturer's protocol of the NASBA kit (Life Science Advanced Technologies Inc., FL, USA) and the reaction products were analyzed according to the same procedure described in 'The NESBA procedure for target gRNA detection'.

RT-PCR

The reverse transcription (RT)-PCR was performed on a C1000™ thermal cycler (Bio-Rad, CA, USA) in a 20 μL solution containing 4 μL reaction buffer for RT (5×), 0.6 μL RevertAid RT (200 U μL^{-1}), 2 μL PCR reaction buffer (10×), 1.4 μL dNTPs (2.5 mM each), 1.4 μL primer set (20 μM each), 0.5 μL i-StarMAX™ II DNA polymerase (5 U μL^{-1}), and 1 μL gRNA solution. T7DNA (NESBA), T7DNA-1 (NESBA), T7DNA-2 (NESBA), and T7DNA (NASBA) were produced by employing a NESBA primer set, NP2 and NASBA primer1, NASBA primer2 and NP1, and a NASBA primer set, respectively. RT was first carried out for 30 min at 50 °C and the PCR was performed for 10 min at 95 °C, followed by 35 cycles of 30 sec at 95 °C, 45 sec at 50 °C, and 60 sec at 72 °C, and further incubation for 5 min at 72 °C. After the completion of the reaction, the RT-PCR products were analyzed by agarose gel electrophoresis. The RT-PCR products were also purified from the product solution by using a Wizard® SV Gel and PCR Clean-Up System (Promega, WI, USA), and their concentrations were determined by using a NanoDrop™ 1000 spectrophotometer (Thermo Fisher Scientific, MA, USA). The purified RT-PCR products were used as markers on lane M1–M4.

Gel electrophoresis

For agarose gel electrophoresis, a 5 μL aliquot of the reaction solution was resolved on 2% agarose gel containing EtBr at a constant voltage of 135 V for 45 min using 1× TBE as the running buffer. Gels were scanned using a UV transilluminator (Bio-Rad, CA, USA).

Target gRNA detection directly from the lysed virus sample

The virus sample (ATCC VR-26 (RSV A), KUMC-42 (RSV B), A/Brisbane/10/2007 (H3N2), A/equine/Kyonggi/SA1/2011 (H3N8), A/California/07/2009 (H1N1), A/swine/Korea/GC0502/2005 (H1N2), and A/aquatic bird/Korea/CN2-MA/2009 (H5N2)) was first thermally lysed by incubating it at 70 °C for 10 min. Then, 1 μL of the lysed solution was added into the NESBA solution (19 μL) instead of 1 μL gRNA solution. The target gRNA included in the lysed virus sample was then analyzed according to the same procedure described in 'The NESBA procedure for target gRNA detection'.

Results and discussion

Overall procedure of the NESBA reaction

The overall procedure of the NESBA reaction is illustrated in Fig. 1. The NESBA reaction basically consists of three reactions denoted as (a), (b), and (c) in Fig. 1: (a) target-induced production of T7 RNA promoter-containing double-stranded DNA (T7DNA), (b) exponential amplification of T7DNA through nicking and extension chain reaction, and (c) transcription-mediated production of RNA amplicons and generation of additional T7DNA from the produced RNA amplicons. The key component underlying the NESBA reaction is a NESBA primer set designed to contain an additional nicking site at the 5′ end of a conventional NASBA primer set consisting of annealing site extended by T7 RNA promoter sequence.

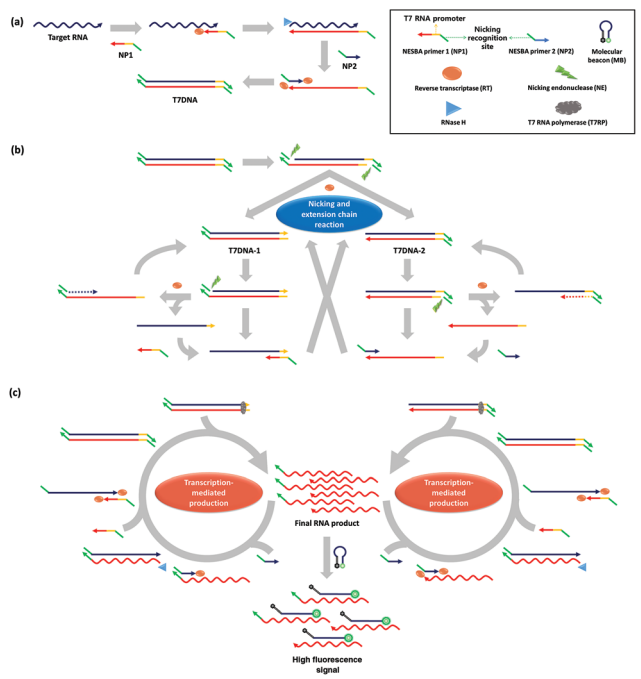

Fig. 1 Schematic illustration of nicking and extension chain reaction system-based amplification (NESBA) for target RNA detection, consisting of (a) target-induced production of T7DNA, (b) exponential amplification of T7DNA through continuously repeated nicking and extension chain reaction, and (c) transcription-mediated production of RNA amplicons and generation of additional T7DNA from the produced RNA amplicons. The arrow indicates the 3′ end of the nucleic acid strand.

In the absence of target RNA, the T7DNA would not be produced and no following NESBA reaction would proceed. In the presence of target RNA, however, NESBA primer 1 (NP1) binds to the target RNA and is extended through reverse transcription promoted by RT, producing a DNA/RNA hybrid. RNase H then degrades the RNA strand in the produced DNA/RNA hybrid leaving extended NP1, to which NESBA primer 2 (NP2) would bind. RT again promotes the extension of the annealed NP2 by an intrinsic DNA polymerase activity, consequently producing T7DNA[42,43] (Fig. 1(a)). This process for target-induced production of T7DNA is exactly the same with that of the NASBA reaction. The T7DNA produced in the NESBA reaction, however, possesses the nicking site at both 5′ ends because a NESBA primer set, NP1 and NP2, contains an additional nicking site at the 5′ ends.

Due to the nicking site at the ends, the produced T7DNA is exponentially amplified through a continuously repeated nicking and extension chain reaction (Fig. 1(b)). Among the several different types of NE, we particularly employed Nt.AlwI because its optimal temperature and working buffer composition are the most compatible with the NESBA reaction (Table S2†). Specifically, Nt.AlwI recognizes the nicking sites in the T7DNA and cleaves one strand generating the 3′ hydroxyl group (OH), from which a new DNA strand is synthesized by RT, producing two types of T7DNAs containing the nicking site at only one end. From the nicking site within the T7DNAs, repeated cycles of nicking, extension, and strand displacement reaction are continuously promoted by the combined activities of NE and RT, consequently producing a large number of T7DNAs. During the extension reaction catalyzed by RT, the cleaved long single-stranded (ss) DNAs are concomitantly displaced to bind to free complementary NP1 or NP2, which enters the nicking and extension chain reaction and further contributes to the exponential amplification of T7DNA.

In the following transcription step, T7RP recognizes the T7 RNA promoter sequence within the T7DNA and catalyzes transcription, producing the final antisense RNA amplicons. The produced RNA amplicons also contribute to the production of T7DNA by binding to NP2 in a similar manner with the original target RNA, further accelerating the production of final RNA amplicons. As a consequence of these combined amplification reactions, a large number of RNA amplicons would be produced. The RNA amplicons could be finally monitored in real-time through the fluorescence signal from the MB probe binding to the amplicons, enabling ultrasensitive detection of target RNA under an isothermal reaction temperature (41 °C).

Feasibility of the NESBA reaction

To prove the feasibility of the proposed method, we conducted the NESBA reaction under various combinations of reaction components by employing respiratory syncytial virus A (RSV A) gRNA as a model target and monitored real-time fluorescence signals produced from the MB binding to the amplified RNA amplicons. As presented in Fig. 2, the highly enhanced fluorescence signal was observed when all the reaction components including a NESBA primer set and NE together with target gRNA were applied (curve 1), whereas no fluorescence signal was observed without target gRNA (curve 2). For comparison, we also conducted the conventional NASBA reaction for the same target (curves 3 and 4). As a result, the NASBA reaction also produced fluorescence signal to some extent from the target, but the signal intensity was quite lower than that from the NESBA reaction because the NASBA reaction is not able to bring about the nicking and extension chain reaction even in the presence of NE (curve 5). In addition, when the NE was omitted from the NESBA reaction, the fluorescence signal was very similar with that of the NASBA reaction (curve 6), confirming that T7DNA is just linearly produced in this case and NE is obviously responsible for the exponential amplification of T7DNA.

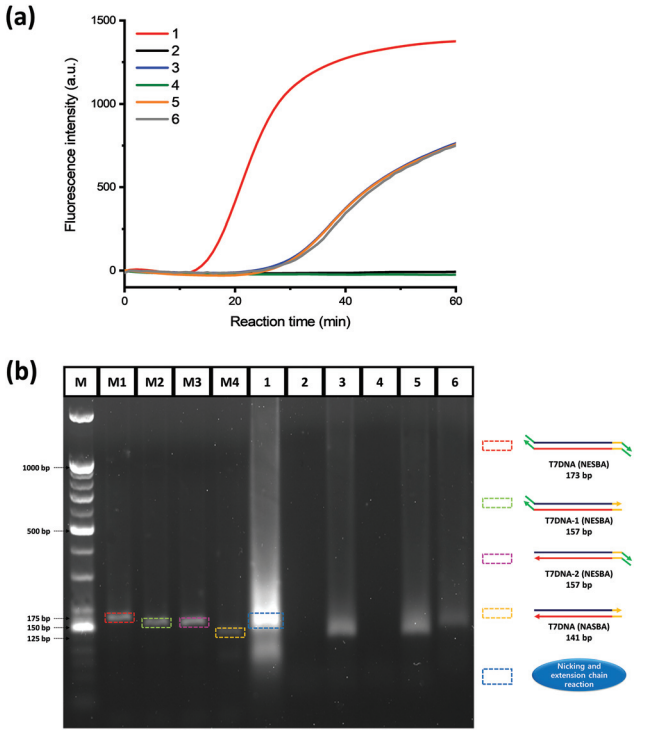

Fig. 2 Feasibility of the NESBA reaction. (a) Time-dependent fluorescence signals produced from the MB during the NESBA reaction. (b) Agarose gel electrophoresis image of the products obtained after 45 min of the NESBA reaction (1: target gRNA + NESBA primer set + NASBA enzyme cocktail + NE, 2: NESBA primer set + NASBA enzyme cocktail + NE, 3: target gRNA + NASBA primer set + NASBA enzyme cocktail, 4: NASBA primer set + NASBA enzyme cocktail, 5: target gRNA + NASBA primer set + NASBA enzyme cocktail + NE, and 6: target gRNA + NESBA primer set + NASBA enzyme cocktail). The final concentrations of target gRNA, NASBA/NESBA primer set, NASBA enzyme cocktail, and NE are 1 pM, 0.7 μM each, 1×, and 0.25 U μL^{-1}, respectively. M1–M4 are markers for the band analysis (M: 25/100 bp mixed DNA ladder, M1: T7DNA (NESBA), M2: T7DNA-1 (NESBA), M3: T7DNA-2 (NESBA), M4: T7DNA (NASBA)). The final concentrations of the markers used for M1–M4 are 100 nM.

We additionally conducted an agarose gel electrophoresis analysis of the products obtained from the NESBA reactions to further support the fluorescence results. For this analysis, we priorly conducted the RT-PCR reactions by employing a NESBA, NESBA/NASBA combined, or NASBA primer set to produce several possible T7DNA intermediate products, which include T7DNA (NESBA) having the nicking site at both ends, T7DNA-1 (NESBA) and T7DNA-2 (NESBA) having the nicking site at only one end, and T7DNA (NASBA) without any nicking site. The produced four T7DNA intermediate products were then employed as markers (M1–M4) for the analysis of the NESBA reaction products. As shown by the results presented in Fig. 2(b), only lane 1 containing all NESBA components (target gRNA, a NESBA primer set, NASBA enzyme cocktail, and NE) showed the bands corresponding to the three key intermediate products of the NESBA reaction including T7DNA (NESBA) (M1), T7DNA-1 (NESBA) (M2), and T7DNA-2 (NESBA) (M3), while none of them was observed without target gRNA (lane 2). On the other hand, the conventional NASBA reaction using a NASBA primer set correctly produced the key intermediate T7DNA product without any nicking site at a slightly lower position only in the presence of target gRNA (lane 3). When NE was additionally added to the NASBA reaction, there was no change observed for the T7DNA product band (lane 5), indicating that not only NE but also a NESBA primer set are needed to produce the intermediate T7DNA products containing the nicking site. Very importantly, the T7DNA product bands obtained from the complete NESBA reaction (lane 1) were much more intensive than those from the NASBA reaction (lane 3) and the incomplete NESBA reactions omitting either a NESBA primer set (lane 5) or NE (lane 6). All these results clearly confirm that the NESBA reaction is properly initiated by target gRNA and both a NESBA primer set containing the nicking site at the 5′ end and NE are quite essential for a highly enhanced amplifying capability of the NESBA reaction, as envisioned in Fig. 1.

Sensitivity of the NESBA reaction

To maximize the efficiency of the NESBA reaction, we optimized various reaction conditions including the concentrations of reaction components (reaction buffers, enzymes, rNTPs, dNTPs, and the NESBA primer set) and reaction temperature by comparing the time-dependent fluorescence signals obtained from the reaction samples with target gRNA to those from the negative control sample without target gRNA. The results showed that 1× NASBA reaction buffer and 0.5× NEBuffer™ 2.1, 1× NASBA enzyme cocktail, 0.25 U μL^{-1} NE, 3.5 mM each rNTP, 0.7 mM each dNTP, 0.7 μM each NESBA primer set, and 41 °C for the reaction temperature are the most optimal for the proposed strategy (Fig. S1–S5†). Thus,

these conditions were used for further experiments in this work.

To determine the sensitivity of the NESBA reaction, target gRNAs at a series of concentrations were subjected to the NESBA reaction and the produced fluorescence signals were measured in a real-time manner. As can be seen in Fig. 3(a), the threshold time (T_t), defined as the time when the fluorescence signal reached the threshold intensity (50 a.u.), gradually decreased as the target gRNA concentration (C_{target}) increased in the range from 1 aM to 1 pM. T_t was then plotted against the logarithm (log) of C_{target} (Fig. 3(b)). As a result, the log of C_{target} showed an excellent linear relationship (T_t = −3.6223 log (C_{target}) − 29.75, R^2 = 0.994) with T_t, confirming that the NESBA reaction is quite capable of quantitatively detecting target gRNA in a real-time manner. The limit of detection (LOD) was estimated to be 1 aM.

For comparison with our strategy, target gRNA at various concentrations was also subjected to the conventional NASBA reaction (Fig. 4). Based on the time-dependent fluorescence signal from the MB probe during the NASBA reaction, we determined T_t for various target concentrations and the obtained T_t was then plotted against the log of C_{target} to determine the LOD. The LOD was estimated to be 100 aM, which is 100-fold higher than that of the NESBA reaction. These results firmly confirm that the proposed NESBA reaction could yield much higher sensitivity than that of the traditional NASBA reaction.

As the NASBA reaction normally requires an initial denaturation step to enhance the amplification efficiency, the developed NESBA reaction also employed the initial denaturation step before the main amplifying reaction. This initial denaturation step, however, might be a critical drawback for the isothermal strategies, and we additionally conducted both the NESBA and NASBA reactions without the initial denaturation step and the reaction products were compared with those from the reactions with the initial denaturation step. As shown by the results presented in Fig. S6,† the elimination of the initial denaturation step slightly diminished the fluorescence signals for both the NESBA and NASBA reactions, but the signal reductions were only marginal, indicating that the initial denaturation is not so critical for the reactions. More importantly, we also observed that the signal reduction due to the omission of the initial denaturation was smaller for the NESBA reaction than the NASBA reaction, indicating that the NESBA reaction is more robustly functional on the target gRNA than the NASBA reaction.

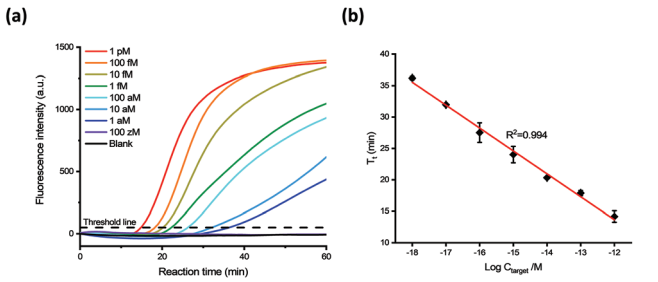

Fig. 3 Sensitivity of the NESBA reaction. (a) Time-dependent fluorescence signals produced from the MB during the NESBA reaction for target gRNA at varying concentrations. (b) The linear relationship between T_t and logarithm of C_{target} in the range from 1 aM to 1 pM, where T_t is defined as the time when the fluorescence signal reached the threshold intensity (50 a.u.) and C_{target} is the concentration of target gRNA.

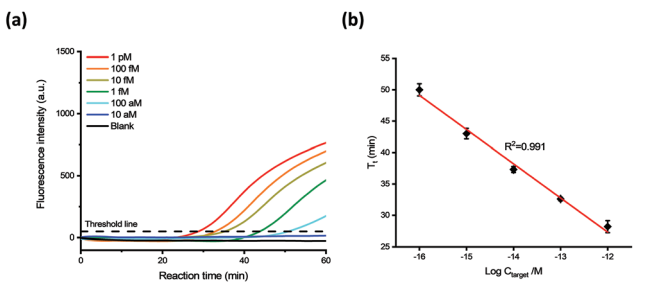

Fig. 4 Sensitivity of the NASBA reaction. (a) Time-dependent fluorescence signals produced from the MB during the NASBA reaction for target gRNA at varying concentrations. (b) The linear relationship between T_t and logarithm of C_{target} in the range from 100 aM to 1 pM, where T_t is defined as the time when the fluorescence signal reached the threshold intensity (50 a.u.) and C_{target} is the concentration of target gRNA.

Specificity of the NESBA reaction

The specificity of the NESBA reaction was next investigated by measuring the time-dependent fluorescence signal from the MB probe during the NESBA reaction for gRNAs extracted from various types of viruses such as RSV A, RSV B, H3N2, H3N8, H1N1, H1N2, and H5N2. As shown by the results in Fig. 5, the highly enhanced fluorescence signal was observed only from the target RSV A gRNA, while the fluorescence signals from the

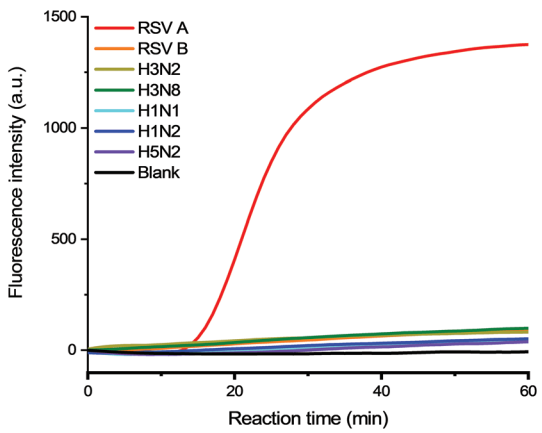

Fig. 5 Specificity of the NESBA reaction. Time-dependent fluorescence signals produced from the MB during the NESBA reaction for gRNAs extracted from various types of viruses such as RSV A, RSV B, H3N2, H3N8, H1N1, H1N2, and H5N2. The concentrations of gRNAs extracted from RSV A and the other viruses are 1 pM and 10 pM, respectively.

non-target samples such as RSV B, H3N2, H3N8, H1N1, H1N2, and H5N2 were very negligible and their intensities were almost the same with that from the negative control without any gRNA even though the non-target gRNAs were employed at 10-fold higher concentration than that of the target RSV A gRNA. Very importantly, even RSV B gRNA having a high sequence homology with RSV A gRNA was also clearly discriminated from the target RSV A gRNA, verifying the excellent capability of the NESBA system to specifically detect the target gRNA against non-specific gRNAs.

Direct detection of target gRNA in lysed virus

Since the integrity of the initial nucleic acids strongly influences the downstream amplification and detection step in molecular diagnostics, the target viral RNA first needs to be extracted from the specimen and undergo purification. In general, silica-based methods such as silica columns[44,45] and silica-coated magnetic beads[46,47] are used to isolate viral RNA from other contaminants after the virus is disrupted. The separate purification step for target nucleic acid, however, would be a great bottleneck, significantly hindering the realization of the fully automated point-of-care (POC) and on-site molecular diagnostics. Therefore, the elimination of the purification step would greatly benefit the molecular diagnostics by simplifying the overall procedures.

Based on this background, we applied the NESBA reaction to detect target gRNA directly from the thermally lysed RSV A virus sample without any gRNA purification step. As shown in Fig. 6(a), the significantly enhanced fluorescence signals were obtained from the target RSV A samples and the signals correctly increased as the virus concentration increased, ranging from 500 to 10^5 $TCID_{50}$ mL^{-1}, which is the typical RSV A concentration range causing bronchiolitis or pneumonia.[48–50] On the other hand, the signals from non-target viruses such as RSV B and H1N1 were very negligible and almost the same with that from the negative control without any virus. The NASBA reaction was also able to identify the target gRNA by producing the fluorescence signal, but its detecting sensitivity was quite lower than that of the NESBA reaction. The results demonstrate that the NESBA reaction is quite robust against PCR inhibiting substances present in biological samples and does not require strict sample purification prior to the amplification, making the NESBA strategy quite promising for POC testing adaptation.

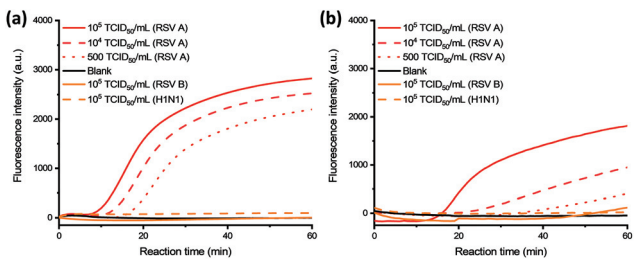

Fig. 6 Detection of target gRNA directly from the lysed virus. Time-dependent fluorescence signals produced from the MB during the (a) NESBA and (b) NASBA reactions for the lysed virus sample at varying concentrations in the range from 500 to 10^5 $TCID_{50}$ mL^{-1}.

Conclusions

We have developed an ultrasensitive version of NASBA utilizing a nicking and extension chain reaction system for target RNA detection termed NESBA. By ingeniously designing a NESBA primer set to contain a nicking site at the 5′ end of a conventional NASBA primer set, the detection sensitivity was significantly enhanced by exponentially amplifying T7DNA produced during the conventional NASBA reaction. The NESBA reaction successfully identified the target gRNA down to 1 aM with an excellent discriminating capability against non-specific gRNAs. The practical utility of this system was further demonstrated by reliable detection of target gRNA directly from the thermally lysed virus sample without any extraction step, confirming its robust applicability in the field of POC and on-site molecular diagnostics.

Conflicts of interest

There are no conflicts to declare.

Acknowledgements

This research was supported by the BioNano Health-Guard Research Center funded by the Ministry of Science and ICT (MSIT) of Korea as Global Frontier Project (Grant Number H-GUARD-2013M3A6B2078964). This research was also supported by the Mid-career Researcher Support Program of the National Research Foundation (NRF) funded by the MSIT of Korea (NRF-2021R1A2B5B03001739).

Notes and references

1 C. A. Holland and F. L. Kiechle, *Curr. Opin. Microbiol.*, 2005, **8**, 504.
2 A. Niemz, T. M. Ferguson and D. S. Boyle, *Trends Biotechnol.*, 2011, **29**, 240.
3 P. Craw and W. Balachandran, *Lab Chip*, 2012, **12**, 2469.
4 T. Notomi, H. Okayama, H. Masubuchi, T. Yonekawa, K. Watanabe, N. Amino and T. Hase, *Nucleic Acids Res.*, 2000, **28**, e63.
5 K. A. Curtis, D. L. Rudolph and S. M. Owen, *J. Med. Virol.*, 2009, **81**, 966.
6 M. M. Parida, S. Sannarangaiah, P. K. Dash, P. V. L. Rao and K. Morita, *Rev. Med. Virol.*, 2008, **18**, 407.
7 S. Cai, C. Jung, S. Bhadra and A. D. Ellington, *Anal. Chem.*, 2018, **90**, 8290.
8 Y.-J. Li and J.-Y. Fan, *BioChip J.*, 2017, **11**, 8.

9 G. T. Walker, M. S. Fraiser, J. L. Schram, M. C. Little, J. G. Nadeau and D. P. Malinowski, *Nucleic Acids Res.*, 1992, **20**, 1691.
10 G. T. Walker, M. C. Little, J. G. Nadeau and D. D. Shank, *Proc. Natl. Acad. Sci. U. S. A.*, 1992, **89**, 392.
11 L. A. Cosentino, D. V. Landers and S. L. Hillier, *J. Clin. Microbiol.*, 2003, **41**, 3592.
12 M. Vincent, Y. Xu and H. Kong, *EMBO Rep.*, 2004, **5**, 795.
13 L. An, W. Tang, T. A. Ranalli, H. J. Kim, J. Wytiaz and H. Kong, *J. Biol. Chem.*, 2005, **280**, 28952.
14 W. Tang, W. H. A. Chow, L. Ying, H. Kong, Y.-W. Tang and B. Lemieux, *J. Infect. Dis.*, 2010, **201**, S46.
15 A. Fire and S. Q. Xu, *Proc. Natl. Acad. Sci. U. S. A.*, 1995, **92**, 4641.
16 P. M. Lizardi, X. Huang, Z. Zhu, P. Bray-Ward, D. C. Thomas and D. C. Ward, *Nat. Genet.*, 1998, **19**, 225.
17 E. J. Cho, L. Yanq, M. Lew and A. D. Ellinqton, *J. Am. Chem. Soc.*, 2005, **127**, 2022.
18 O. Piepenburg, C. H. Williams, D. L. Stemple and N. A. Armes, *PLoS Biol.*, 2006, **4**, 1115.
19 S. Lutz, P. Weber, M. Focke, B. Faltin, J. Hoffmann, C. Müller, D. Mark, G. Roth, P. Munday, N. Armes, O. Piepenburg, R. Zengerle and F. Von Stetten, *Lab Chip*, 2010, **10**, 887.
20 C. Jung, J. W. Chung, U. O. Kim, M. H. Kim and H. G. Park, *Anal. Chem.*, 2010, **82**, 5937.
21 C. Jung, J. W. Chung, U. O. Kim, M. H. Kim and H. G. Park, *Biosens. Bioelectron.*, 2011, **26**, 1953.
22 J. Van Ness, L. K. Van Ness and D. J. Galas, *Proc. Natl. Acad. Sci. U. S. A.*, 2003, **100**, 4504.
23 E. Tan, B. Erwin, S. Dames, K. Voelkerding and A. Niemz, *Clin. Chem.*, 2007, **53**, 2017.
24 J. Compton, *Nature*, 1991, **350**, 91.
25 M. L. Landry, R. Garner and D. Ferguson, *J. Clin. Microbiol.*, 2005, **43**, 3136.
26 C. Ong, W. Tai, A. Sarma, S. M. Opal, A. W. Artenstein and A. Tripathi, *J. Mol. Diagn.*, 2012, **14**, 206.
27 J. Y. Song, Y. Jung, S. Lee and H. G. Park, *Anal. Chem.*, 2020, **92**, 10350.
28 H. Y. Kim, J. K. Ahn, C. Y. Lee and H. G. Park, *Anal. Chim. Acta*, 2020, **1114**, 7.
29 S. Lee, H. Jang, H. Y. Kim and H. G. Park, *Biosens. Bioelectron.*, 2020, **147**, 111762.
30 C. R. Park, S. J. Park, W. G. Lee and B. H. Hwang, *Biotechnol. Bioprocess Eng.*, 2018, **23**, 355.
31 A.-M. Vandamme, S. Van Dooren, W. Kok, P. Goubau, K. Fransen, T. Kievits, J.-C. Schmit, E. De Clercq and J. Desmyter, *J. Virol. Methods*, 1995, **52**, 121.
32 S. A. Simpkins, A. B. Chan, J. Hays, B. P. öpping and N. Cook, *Lett. Appl. Microbiol.*, 2000, **30**, 75.
33 S. A. Burchill, L. Perebolte, C. Johnston, B. Top and P. Selby, *Br. J. Cancer*, 2002, **86**, 102.
34 J. M. Yang, K. R. Kim and C. S. Kim, *Biotechnol. Bioprocess Eng.*, 2018, **23**, 371.
35 R. S. Lanciotti and A. J. Kerst, *J. Clin. Microbiol.*, 2001, **39**, 4506.
36 L.-T. Lau, J. Banks, R. Aherne, I. H. Brown, N. Dillon, R. A. Collins, K.-Y. Chan, Y.-W. W. Fung, J. Xing and C. Albert, *Biochem. Biophys. Res. Commun.*, 2004, **313**, 336.
37 B. Deiman, C. Schrover, C. Moore, D. Westmoreland and P. Van de Wiel, *J. Virol. Methods*, 2007, **146**, 29.
38 Q. Wu, C. Suo, T. Brown, T. Wang, S. A. Teichmann and A. R. Bassett, *bioRxiv*, 2020.
39 S. Gayathri, S. Mounika, K. Banu, B. Rai and B. Mondal, *Glob. J. Clin. Virol.*, 2020, **5**, 1.
40 N. Cook, *J. Microbiol. Methods*, 2003, **53**, 165.
41 B. Deiman, P. van Aarle and P. Sillekens, *Mol. Biotechnol.*, 2002, **20**, 163.
42 E. Gilboa, S. W. Mitra, S. Goff and D. Baltimore, *Cell*, 1979, **18**, 93.
43 A. Telesnitsky and S. P. Goff, *EMBO J.*, 1993, **12**, 4433.
44 L. Li, X. Deng, E. T. Mee, S. Collot-Teixeira, R. Anderson, S. Schepelmann, P. D. Minor and E. Delwart, *J. Virol. Methods*, 2015, **213**, 139.
45 G. Rohde, A. Wiethege, I. Borg, M. Kauth, T. Bauer, A. Gillissen, A. Bufe and G. Schultze-Werninghaus, *Thorax*, 2003, **58**, 37.
46 N. Sun, C. Deng, Y. Liu, X. Zhao, Y. Tang, R. Liu, Q. Xia, W. Yan and G. Ge, *J. Chromatogr. A*, 2014, **1325**, 31.
47 M. G. Milia, T. Allice, G. Gregori, S. Mussino, G. Orofino, S. Bonora and V. Ghisetti, *J. Clin. Virol.*, 2010, **47**, 8.
48 C. B. Hall, R. Douglas, K. C. Schnabel and J. M. Geiman, *Infect. Immun.*, 1981, **33**, 779.
49 J. Mills, J. E. Van Kirk, P. F. Wright, R. M. Chanock and I. E. Fishburne, *J. Immunol.*, 1971, **107**, 123.
50 D. A. Tristram, R. W. Miller, J. A. McMillan and L. B. Weiner, *Am. J. Dis. Child.*, 1988, **142**, 834.